J Electroanal Chem, 146 (1983) 93–108
Elsevier Sequoia S.A., Lausanne – Printed in The Netherlands

CHANGES IN THE ELECTROCHEMICAL RESPONSE OF NOBLE METALS PRODUCED BY SQUARE-WAVE POTENTIAL PERTURBATIONS

A NEW TECHNIQUE FOR THE PREPARATION OF REPRODUCIBLE ELECTRODE SURFACES OF INTEREST IN ELECTROCATALYSIS

A.C. CHIALVO, W.E. TRIACA and A J. ARVIA

Instituto de Investigaciones Fisicoquímicas Teóricas y Aplicadas, (INIFTA), División Electroquímica, Sucursal 4 — Casilla de Correo 16, (1900) La Plata (Argentina)

(Received 16th April 1982; in revised form 21st September 1982)

ABSTRACT

A square-wave potential anodizing procedure to obtain noble metal surfaces with both a controlled roughness and a reproducible electrochemical response is presented. The influence of the characteristics of the square-wave potential perturbation are systematically studied. The modification of the surface takes place through the formation of a hydrated platinum oxide layer which is later electroreduced. The mechanism of growth of the hydrated oxide layer under both square-wave potential perturbation and potentiostatic conditions is critically discussed in terms of a complex sandwich-type structure.

INTRODUCTION

Many works have been published on the anodization at high potential values of platinum metal electrodes, using both dc and ac biased with dc [1–33]. Under these conditions an oxide multilayer on the electrode surface is apparently formed. The structure of the multilayer was interpreted in terms of two distinguishable types of oxides (OxI and OxII) [18,19,26,28]. The characteristic of the electrochemical reduction of the thick oxide layers has also been investigated under different experimental conditions including the influence of anions [32,33]. In terms of the electroreduction of the aged O-species, these results indicate that there is a limiting oxygen coverage on smooth Pt anodes in acid electrolytes [5,13,17].

From a critical reversion of published results one concludes that most of them were obtained under experimental conditions which are not straightforwardly comparable and, except for the works of James [12] and Shibata and Sumino [18], little attention has been paid to the change in the electrode roughness during the anodic polarization. The latter is a relevant aspect when the electrodes are intended for application in electrocatalysis. On the other hand, the most recent works related to the O-electroadsorption and electrodesorption on noble metals [34,35] point out that the conventional idea of bulk stoichiometry hydration state and stability of the

0022-0728/83/$03 00

film-forming species at those electrode surfaces have to be more critically considered to evaluate their corresponding electrocatalytic properties.

Recent studies on the potentiodynamic electroformation and electroreduction of O-containing species on noble metals reveal that surface restructuring plays an important role, especially when the electrode potential is repeatedly changed between certain limits associated with the potential range where the potentiodynamic ageing effects are observed [36,37]. Under these circumstances the penetration of oxygen within the first layers of the metal lattice is feasible through the dynamic behaviour of both the oxygen atoms and the platinum atoms located mainly at the first metal lattice planes. Consequently, under the above-mentioned conditions, the characteristics of the overall potentiodynamic E/I profile in the potential range of thermodynamic stability of bulk water changes remarkably. These results suggest the possibility of changing more drastically the structural characteristics of the metal surface by means of a periodic potential perturbation covering a positive potential limit exceeding that usually assigned to the O-monolayer electroformation on noble metals. This possibility is sustained by the fact that when platinum is strongly anodized it becomes covered by an oxide film and simultaneously oxygen dissolves in the bulk metal [11,31]. Similar results are obtained when platinum is chemically oxidized in oxygen-saturated concentrated nitric acid [38,39]. In this case it was concluded that a Pt–O alloy is formed and the structure of the latter is maintained, even when dissolved oxygen has been removed by extended periods of strong cathodization in hydrogen-saturated acid solutions.

This report describes a new procedure to obtain noble metal surfaces involving both a controlled roughness and a reproducible electrochemical response. This is achieved by perturbing the electrode with a square-wave potential signal under carefully chosen conditions.

EXPERIMENTAL

Runs were made in a three-electrode compartment Pyrex glass cell, the counter-electrode compartment being connected directly to the rest of the cell to minimize the ohmic drop between the electrodes. Most of the runs were made with platinum working electrodes. However, rhodium and gold working electrodes were also used to investigate the possible generalization of the treatment to other noble metals. The working electrodes were either in the form of wires (4–6 mm long and 0.5 mm diam.) or plates (2×6 mm). Previous to each experiment they were electropolished with ac (50 Hz; 10–15 V) in a slightly acid (HCl) saturated $CaCl_2$ solution. Later the electrodes were repeatedly rinsed with triply distilled water and finally immersed for 1 h in an electrolyte solution similar to that employed in the cell to facilitate the desorption of chloride ions. The potentiodynamic behaviour of the treated electrodes in the 0.01–1.4 V range was very reproducible. A platinum counterelectrode and a hydrogen reference electrode in the same solution were employed. Runs were made in different acid electrolytes (0.5 M H_2SO_4 and 1 M $HClO_4$) at 30°C. Solutions were prepared with triply distilled water free of organic impurities.

The initial true electrode area was evaluated through the H-adatom monolayer charge resulting from conventional potentiodynamic profiles run with triangular potentials sweeps (TPS) at 0.3 V s^{-1} between 0.01 and 1.40 V. Afterwards, the electrode was subjected to a square-wave potential signal (SWPS), whose switching potentials (E_u and E_l) were preselected accordingly to the purpose of each run. The upper switching potential was located in the range where the growth of the oxide film takes place.

RESULTS

Voltamperometric characteristics of a platinum electrode after applying the square-wave potential signal.

The potentiodynamic E/I profiles obtained with the Pt/0.5 M H_2SO_4 interface at 30°C under a repetitive triangular potential sweep (RTPS) after 5 min cycling at 0.3 V s^{-1} (Fig. 1a) exhibit in the 0.01–1.40 V range the conventional current contributions related to the electroadsorption and electrodesorption of the H- and O-monolayers described in the literature [34]. The conventional complex O-electrodesorption current peak appears at ca. 0.75 V. The profile shown in Fig. 1a is useful for comparison with that obtained with the same interface after the electrode has been subjected to the SWPS ($E_u = 2.40$ V, $E_l = 0.4$ V, period $\tau = 560$ μs and duration $t = 3$ min). Within the 0.4–2.4 V range there is a net growth of a hydrated platinum oxide film and the electrode surface acquires a net brown-yellow colour. When the hydrated platinum oxide is dried under a nitrogen atmosphere at 30°C, its colour turns to dark brown and its apparent volume is reduced by a factor of ca. 10. The potentiodynamic electroreduction profile of the hydrated platinum oxide film run immediately after the SWPS treatment exhibits a relatively thin cathodic current peak at ca. 0.15 V (Fig. 1b), the corresponding charge being ca. 18 mC cm^{-2}. The electroreduction of the hydrated oxide film yields a net increase in the electrode surface area (Fig. 1c). The corresponding RTPS voltammogram is to some extent similar to that illustrated in Fig. 1a, but the charges both anodic and cathodic involved are appreciably increased. The relative actual increase in the electrode real surface area (R) can be evaluated through the relationship

$$R = (Q_H)_a/(Q_H)_b \quad (1)$$

where Q_H represents the H-electroadsorption monolayer charge before (b) and after (a) the SWPS is applied. In the sequence of runs shown in Fig. 1, $R = 22.6$. The potentiodynamic response of the electroreduced platinum surface after the SWPS treatment is very close to that reported for platinized platinum electrodes. However, the electrodes subjected to SWPS treatment present a mirror-like aspect, in contrast with the dull surface of platinized platinum.

The fresh hydrated platinum oxide film exhibits a gel-like-type aspect. The scanning electron micrographs obtained after dehydration of the gel-like-type film appear with a cracked structure (Fig. 2). The X-ray diffractogram of the hydrated

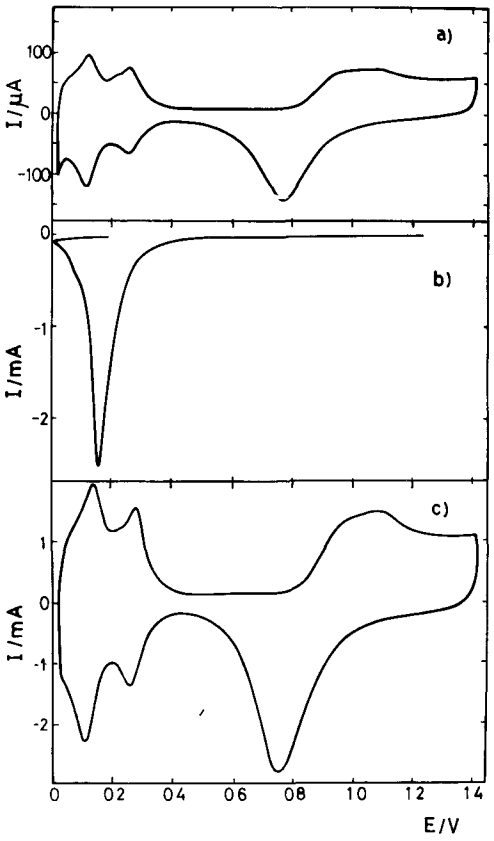

Fig 1 Potentiodynamic E/I profiles run with 0 5 M H_2SO_4 at 30°C. (a) Platinum electrode without SWPS treatment after 5 min cycling at 0.3 V s^{-1}, (b) electroreduction profile at 3×10^{-3} V s^{-1} immediately after the SWPS treatment (E_u = 2 4 V, E_l = 0.4 V, τ = 560 μs, t = 3 min), (c) electroreduced platinum after 5 min cycling at 0 3 V s^{-1}

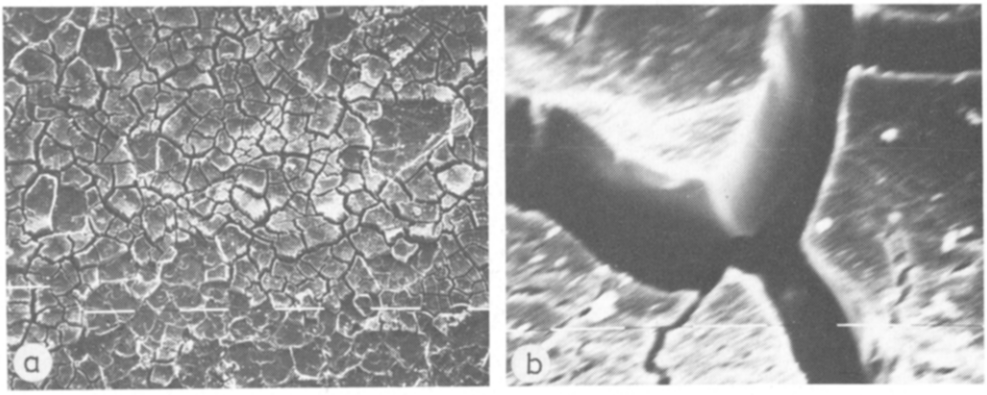

Fig. 2. Scanning electron micrographs of hydrated platinum oxide obtained after the SWPS treatment (E_u = 2.4 V, E_l = 0 V, τ = 560 μs, t = 3 min, 0 5 M H_2SO_4, 30°C) Magnification (a) 100×, (b) 1600×

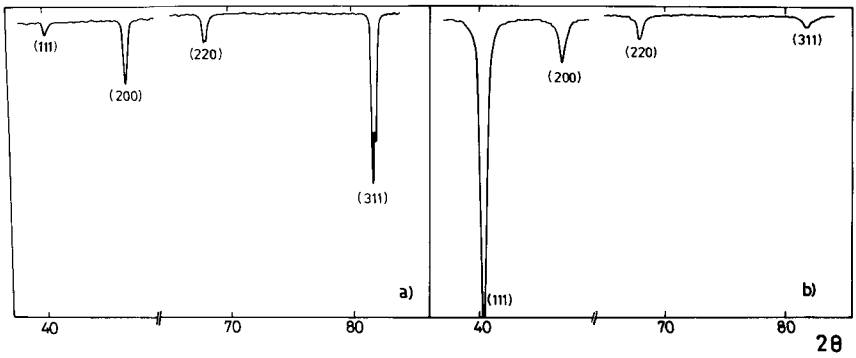

Fig. 3. X-ray diffractograms obtained with (a) untreated platinum electrode, (b) electroreduced platinum surface after the SWPS treatment ($E_u = 2\,4$ V, $E_l = 0$ V, $\tau = 560$ μs, 0 5 M H_2SO_4, 30°C)

platinum oxide formed after the SWPS treatment indicates an apparent amorphous structure.

The X-ray diffractograms (from 5° to 90°) were obtained under two well-defined conditions (Fig. 3): (1) the untreated platinum electrode (trace a); (2) the electrode which was subjected to the SWPS treatment and electroreduced by an immediatly following negative-going potential sweep (trace b). Trace (a) shows the peaks of pure polycrystalline platinum. They correspond to reflexions from the (111), (200), (220) and (311) planes [40]. Trace (b) shows a remarkable intensity increase of the peak related to the (111) plane. Comparison of the two diffractograms suggests that the electroreduced platinum surface after the SWPS treatment, results in an additional preferred orientation.

Platinum peaks are missing in the X-ray diffractograms corresponding to the hydrated platinum oxide, except for a relatively weak contribution of the reflexion of

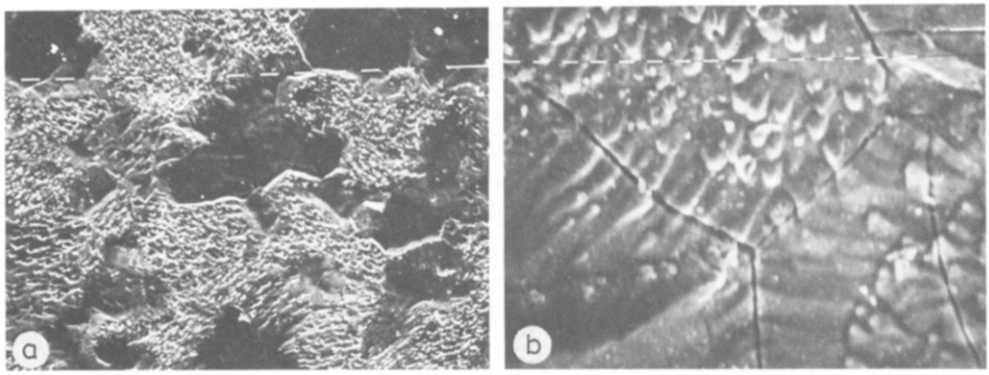

Fig 4 Scanning electron micrographs of an electroreduced platinum surface after SWPS treatment ($E_u = 2\,4$ V, $E_l = 0$ V; $\tau = 560$ μs, $t = 3$ min; 0.5 M H_2SO_4, 30°C) Magnifications (a) 400×, (b) 3200×.

the (111) plane, probably due to a partial decomposition of the hydrated platinum oxide.

The topography at different magnifications of the electroreduced platinum surface after the SWPS treatment was observed. At low magnification (Fig. 4a) a sponge-like structure over the entire surface is observed. At higher magnification (Fig. 4b) the surface exhibits two main characteristics: (1) the occurence of patches which are separated by grooves; (2) the appearance of macro-stepped-like surface regions in each patch.

No platinum ionic species in the electrolyte was detected by the atomic absorption technique even after subjecting the electrode to the SWPS treatment for 4 h ($E_u = 2.4$ V, $E_l = 0$ V, $\tau = 560$ μs).

Dependence of the electroreduction charge of the hydrated platinum oxide on the characteristics of the SWPS

The electroreduction charge related to the hydrated platinum oxide (Q_r) recorded after the SWPS treatment can be taken as a measure of the platinum real surface area (S) (Fig. 5). For the evaluation of S the H-adatom monolayer charge was taken into account as referred to above. Under a constant set of perturbation conditions Q_r depends on the duration time of the SWPS (Fig. 6). Likewise, the potential of the peak related to the electroreduction of the hydrated platinum oxide shifts towards lower potential values as the duration time of the SWPS increases. The corresponding complex electroreduction E/I profile starts at ca. 0.65 V, both in 0.5 M H_2SO_4

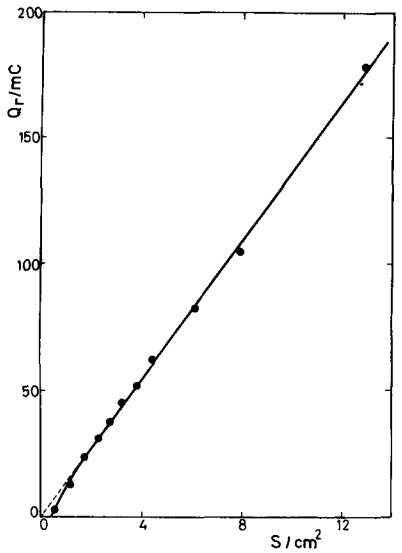

Fig. 5. Relationship between Q_r and the electroreduced platinum surface area after SWPS treatment ($E_u = 2.4$ V; $E_l = 0$ V; $\tau = 560$ μs, 0.5 M H_2SO_4, 30°C)

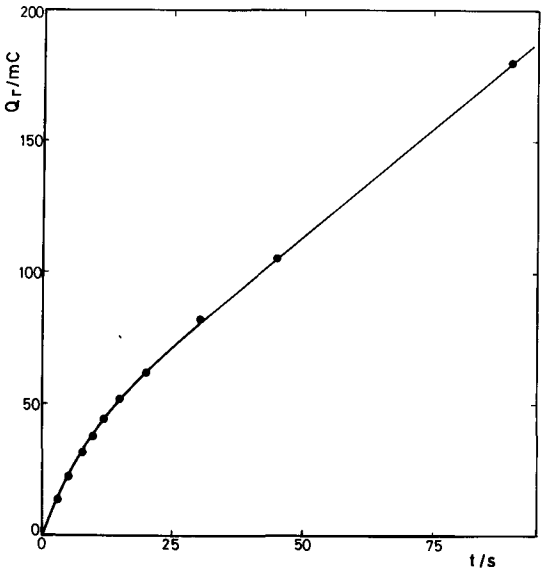

Fig 6. Dependence of Q_r on t SWPS characteristics. $E_u = 2.4$ V, $E_l = 0$ V, $\tau = 560$ μs 0 5 M H_2SO_4, 30°C

and in 1 M $HClO_4$. There is, however, a slight influence of the electrolyte composition in the overall electrochemical behaviour which apparently manifests itself in the rate of hydrated platinum oxide growth under the SWPS treatment.

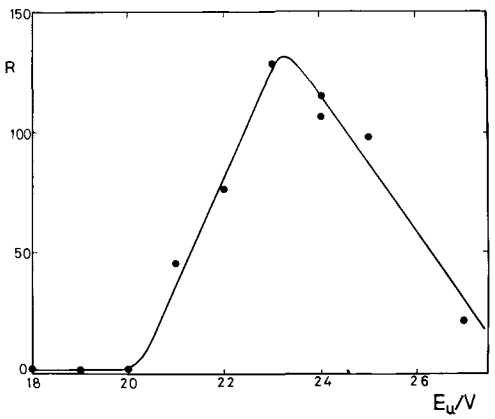

Fig. 7 Dependence of R on E_u. SWPS characteristics: $E_l = 0$ V, $\tau = 560$ μs, $t = 5$ min. 0 5 M H_2SO_4, 30°C.

Influence of the SWPS characteristics on the increase of real surface area of platinum electrodes

The value of R changes with E_u according to a volcano-shaped curve (Fig. 7). Under a definite set of perturbation conditions in both 0.5 M H_2SO_4 and 1 M $HClO_4$ the maximum R value is obtained at ca. 2.3 V. The curve exhibits a threshold potential located at ca. 2.0 V for the occurrence of the real surface area increase. The shape of the curve is independent of both E_l (-0.3 V $\leqslant E_l \leqslant 0.5$ V) and τ (0.1 ms $\leqslant \tau \leqslant 2$ ms). The threshold potential coincides with that reported in the literature for the potentiodynamic growth of the platinum oxide layer in acid electrolytes [18,19,22]. A similar volcano-shaped relationship is found between R and E_l (Fig. 8), the maximum value of R being located at ca. 0 V. In this case, the shape of the curve is independent of both E_u (2.0 V $\leqslant E_u \leqslant 2.8$ V) and τ (0.1 ms $\leqslant \tau \leqslant 2$ ms).

For a symmetrical SWPS under preset E_u and E_l values there is a frequency ($f = 1/\tau$) associated with the maximum value of R (Fig. 9). Accordingly, the optimal range of τ extends from 0.2 to 0.4 ms. This optimal range of τ is, in principle, independent of both E_u and E_l. Furthermore, the value of R depends on the duration time of the SWPS (Fig. 10). Initially R increases linearly with t, and a maximum R value is obtained at $t \approx 4$ min. Then R decreases with t, probably because of the partial detachment of the oxide film. Under these circumstances an accumulation of the product at the bottom of the cell is noticed.

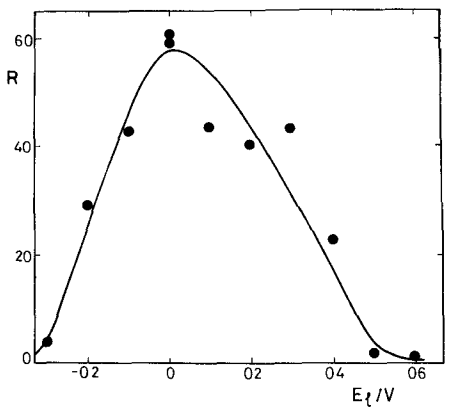

Fig. 8. Dependence of R on E_l SWPS characteristics $E_u = 2.4$ V; $\tau = 560$ μs, $t = 3$ min 0.5 M H_2SO_4, 30°C

DISCUSSION

It has been known for a long time that the ac electrooxidation of platinum electrodes yields $PtO_2 \cdot n\ H_2O$ [1,7,20], the product being found to be amorphous by X-ray analysis [1,6,20]. The growth of the oxide layer is accelerated when the

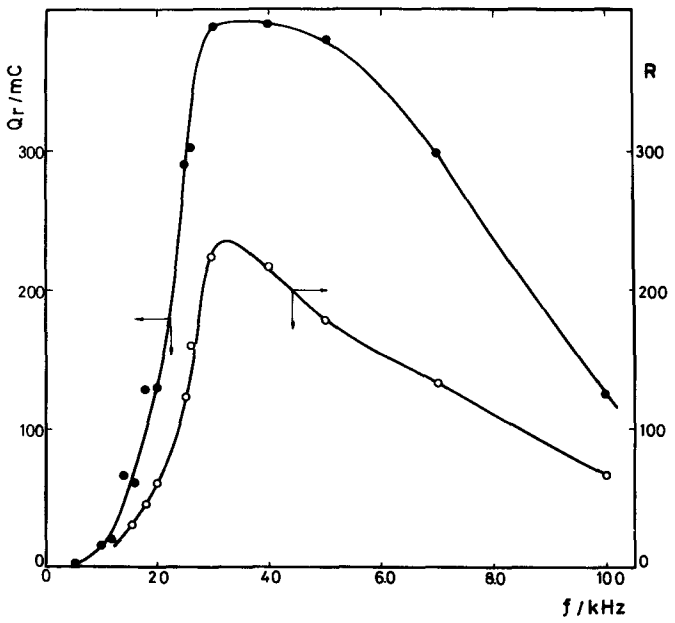

Fig. 9 Dependence of Q_r and R on f. SWPS characteristics: $E_u = 2.4$ V, $E_l = 0$ V, $t = 2$ min. 0 5 M H_2SO_4, 30°C

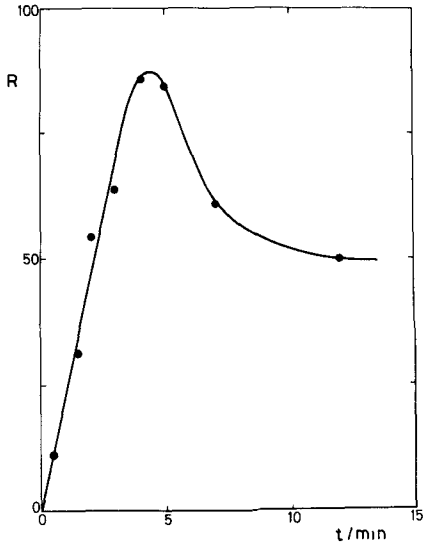

Fig. 10. Dependence of R on t. SWPS characteristics: $E_u = 2.2$ V; $E_l = 0$ V; $\tau = 400$ μs. 0 5 M H_2SO_4; 30°C

electrolysis is carried out by ac superimposed on dc [1,20]. The yellow-coloured product exhibits an electroreduction current peak at ca. 0.2 V [19,26,32]. The rate of formation of phase platinum oxide in 0.5 M H_2SO_4 at 2.3 V diminishes with the increase in H_2SO_4 concentration [19] and also depends on the ionic composition of the solution [22], temperature [18,26] and metallographic characteristics of the base metal [12,19].

The present results demonstrate that the modification of the active surface and the increase in the real surface area of platinum electrodes is produced by the electroreduction of the hydrated oxide layer generated by the SWPS treatment. To produce the increase in the real surface area the ranges of the SWPS characteristics, for the electrolytes used in this work, at 30°C are: 2.0 V $\leqslant E_u \leqslant$ 2.8 V, -0.3 V $\leqslant E_l \leqslant 0.5$ V and 0.1 ms $\leqslant \tau \leqslant 2$ ms. Within the useful E_u potential range no soluble platinum species is detected, in agreement with previous results related to the potentiostatic growth of platinum oxide in acid electrolyte [18]. This result, however, does not rule out the possibility that during each cycle of the SWPS treatment, the electrodissolution of platinum takes place when $E_u > 2.0$ V and the electrodeposition occurs at $E_l < 0.5$ V. In this sense, the SWPS perturbation technique gives no direct evidence of such processes, as in the case of triangular potential cycling [34].

From the kinetic standpoint there is a remarkable difference when the increase of R occurs either under SWPS or under potentiostatic conditions. Under the preset conditions of Fig. 10, R reaches a value > 75 in 3–5 min, while the value of R resulting by holding the electrode potential at 2.4 V for 3 h is about 5. This difference indicates that the corresponding hydrated oxide film growth mechanism in each case is probably different. Therefore, the two important aspects to be considered are the structural changes of the platinum surface promoted by the SWPS treatment and the possible reactions of the hydrated oxide film growth, to envisage the participation of the different species which, during the electroreduction, are responsible for the real surface area increase.

The increase in R and the structural changes of the platinum surface are only observed after the thick, anodically formed hydrated platinum oxide layer has been electroreduced. The hydrated nature of the oxide film is immediately derived from the scanning electron micrographs obtained after drying the electrode surface. The amorphous hydrated platinum oxide can be represented as a $PtO_n \cdot x\ H_2O$ species, where $2 \leqslant n \leqslant 3$ and x is unknown.

The electroreduction of the hydrated oxide layer can be written according to the overall reaction

$$PtO_n \cdot x\ H_2O + 2n\ e + 2\ n\ H^+ \rightarrow Pt + (x + n)\ H_2O \qquad (2)$$

After the electroreduction process, the platinum atoms should remain in a metastable structure related to both the surface area increase and the predominant contribution of the (111) planes parallel to the metal surface. This should correspond to a preferential orientation of grains which originates a textured metal surface. Therefore, the textured platinum electrode should be considered to be a different electrode material from either conventional bright platinum or platinized platinum. Pre-

liminary experiments indicate that the electrocatalytic activity of the textured platinum for the electrochemical oxidation of ethylene is appreciably higher than that corresponding to the conventional platinized platinum electrodes [41]. This fact might be to some extent related to the enhancement of the electrocatalytic activity of platinum for electrochemical reductions when the electrodes are subjected to anodic polarization followed by reduction [20].

The mechanism of the increase of the platinum real surface area can envisaged through the growth mechanism of the oxide layer formation on the basis of the following facts associated with the SWPS treatment.

(1) The existence of the E_u threshold potential which coincides with the standard potential of the equilibrium [42]

$$PtO_2 + H_2O = PtO_3 + 2\,H^+ + 2\,e, \qquad E^0 = 2.0\ V \tag{3}$$

This agreement, however only serves to indicate that a higher platinum oxide is probably involved in the process since there is no clear evidence of the existence of PtO_3. Furthermore, the upper limit of E_l lies in the potential range where the electrooxidation of water according to the formal reaction

$$Pt + H_2O = Pt(OH) + H^+ + e \tag{4}$$

takes place.

(2) The SWPS frequency range related to the maximum efficiency in the increase of the real surface area.

(3) The minor influence of the solution composition in the overall effect.

(4) The occurrence of various oxygen-containing species during the oxide film formation when the film is produced, either by the SWPS technique or by holding the potential at high positive values. In the former case, the electroreduction E/I profile corresponding to the potential region preceding the electroreduction of the hydrated oxide layer, reveals a small cathodic hump at 0.82 V, the corresponding charge being less than that of the O-monolayer on platinum (Fig. 11a). This potential is ca. 0.05 V more positive than that of the conventional RTPS electroreduction current peak associated with the non-aged O-containing monolayer under comparable experimental conditions. Therefore, as in the former case the reactant should be more unstable than in the latter, it suggests that the O-containing monolayer is located above a platinum–oxygen–like alloy substrate instead of a bare platinum surface. This assumption is confirmed by the appearance of a net cathodic peak at ca. 0.59 V which coincides with the peak obtained after the potentiostatic electrooxidation of platinum at 2.4 V (Fig. 11b). The charge related to this current peak reaches a limiting value of ca. 1 mC real cm^{-2} which is probably related to that corresponding to the electroreduction of oxygen located within the first layers of the metal lattice [36,37].

The electroreduction E/I profile run after holding the potential at 2.4 V for 1 s (Fig. 11b) is similar to that obtained after the SWPS treatment except for the absence of the small hump at ca. 0.8 V. Thus, Fig. 11b shows the occurrence of a current peak also located at ca. 0.59 V, the corresponding charge being 1.1 mC real cm^{-2}.

The activity of the platinum electrode, which is usually assigned to dissolved oxygen in the metal during anodizing, should be primarily associated with the expansion of the metal lattice during the anodic or the anodic–cathodic potential

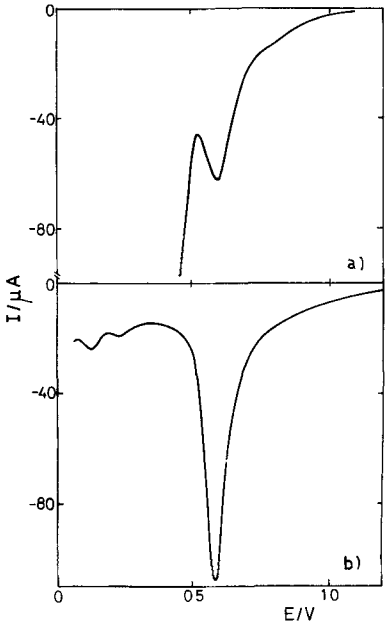

Fig. 11. Potentiodynamic E/I profiles run at 0.3 V s^{-1} with 0 5 M H_2SO_4 at 30°C (a) after the SWPS treatment ($E_u = 2.4$ V, $E_l = 0$ V; $\tau = 400$ μs, $t = 1$ s); (b) after holding the potential at 2 4 V for 1 s.

treatment which facilitates oxygen penetration into the metal, at least in the order of a few metal layers [36]. Nevertheless, as recently pointed out, a dissolved oxygen atom can be interstitially located in the octahedral hole in the centre of the unit platinum crystal face centre cube and produces a lattice expansion [31], as observed in X-ray diffraction analysis. There is evidence of intergranular oxygen atoms in platinum obtained from oxygen diffusion studies in the metal [10,25].

The structure of the complex interphase resulting after the SWPS treatment is depicted in Fig. 12. On the basis of this structure the formation of the sandwich-type interphase can be described in terms of various reaction stages which take into account the characteristics of the oxygen-containing monolayers and multilayers on platinum already discussed in the literature [34–37] and the possibility of high oxidation states of platinum in the oxygen evolution potential range. The following stages are postulated:

(1) Oxygen-containing monolayer formation:

$$Pt + H_2O = Pt(OH) + H^+ + e \qquad (5)$$

$$Pt(OH) = Pt(O) + H^+ + e \quad (6)$$

$$Pt(O) = Pt(O)_{aged} \quad (7)$$

Reaction (5) is a fast process which behaves in a reversible way [43]. According to previous measurements a significant relaxation effect in the behaviour of the OH intermediate at 25°C in 1 *M* H_2SO_4, as deduced from the triangular modulated triangular potential sweeps, occurs at 500 Hz [43], a figure which is in the frequency range of the SWPS which corresponds to the initiation of the oxide film growth. This means that under preset E_u and E_l values at the SWPS frequency corresponding to the maximum efficiency, the greatest coupling between the potential perturbation and the kinetics of reaction (5) is achieved. Therefore, the Pt(OH) species should be considered as the starting material for producing the hydrated platinum oxide layer. Reactions (6) and (7) were discussed in the O-electroadsorption process on platinum [36,37].

(2) Layer 1 formation:

$$[Pt]Pt(O)_{aged} = [Pt](\text{layer } 1) \quad (8)$$

Reaction (8) corresponds to the formation of an oxygen–platinum-like alloy (layer 1) involving a limiting thickness of about two or three layers. The formation of such layers has also been investigated by means of potentiodynamic ageing techniques [36,37]. The electrodissolution of platinum probably occurs through the aged O-containing monolayer.

(3) Layer 2 formation:

$$[Pt](\text{layer } 1) \underset{H^+, e}{\overset{H_2O}{=}} [Pt](\text{layer } 1)(\text{layer } 2)^{\star} \quad (9a)$$

$$[Pt](\text{layer } 1)(\text{layer } 2)^{\star} = [Pt](\text{layer } 1)(\text{layer } 2) \quad (9b)$$

Reaction (9a) involves the participation of the surface platinum atoms of layer 1 and

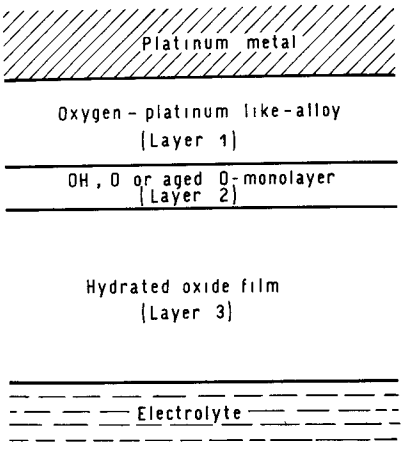

Fig. 12 Scheme of the structure of the complex sandwich-type interphase.

corresponds to the formation of a non-stabilized oxygen-containing monolayer (layer 2)* on layer 1, while reaction (9b) yields an aged oxygen-containing monolayer (layer 2).

(4) Hydrated oxide film formation:

$$[Pt](\text{layer 1})(\text{layer 2})^{\star} \underset{H^+, e}{\overset{H_2O}{=}} [Pt](\text{layer 1})(\text{layer 2})^{\star}(\text{layer 3}) \quad (10a)$$

$$[Pt](\text{layer 1})(\text{layer 2}) \underset{H^+, e}{\overset{H_2O}{=}} [Pt](\text{layer 1})(\text{layer 2})(\text{layer 3}) \quad (10b)$$

Therefore, the formation of the hydrated platinum oxide layer (layer 3) can occur either from an oxygen–platinum-like alloy layer covered by a non-aged oxygen monolayer (reaction 10a) or from an oxygen–platinum-like alloy covered with an aged oxygen monolayer (reaction 10b).

(5) Hydrated oxide film growth and oxygen evolution:

$$[Pt](\text{layer 1})(\text{layer 2})^{\star}(\text{layer 3}) \underset{H^+, e}{\overset{H_2O}{=}} [Pt](\text{layer 1})(\text{layer 2})^{\star}(\text{layer 3}) + O_2 \quad (11a)$$

$$[Pt](\text{layer 1})(\text{layer 2})(\text{layer 3}) \underset{H^+, e}{\overset{H_2O}{=}} [Pt](\text{layer 1})(\text{layer 2})(\text{layer 3}) + O_2 \quad (11b)$$

Thus, the growth of layer 3 takes place simultaneously with the evolution of oxygen according to the global reactions (11a) or (11b).

Taking into account that the potential range associated with the initiation of the growth process coincides with the thermodynamic potential of the PtO_2/PtO_3 couple, according to reaction (3), and the fact that film growth occurs simultaneously with oxygen evolution, both reactions can take place, probably through the formation of an intermediate involving a higher platinum oxide. These reaction intermediates either decompose yielding molecular oxygen, or through a redox process occurring in the film contribute to the film growth process. The former possibility is sustained by the kinetic studies of the oxygen evolution reaction on platinum electrodes at high anodic potentials [9,44].

The preceding discussion indicates that stages (5)–(8), (9a), (10a) and (11a) predominate during the SWPS treatment. This means that the unstable forms of the oxygen-containing species are in this case mainly responsible for the film growth process. The overall reaction implies a dynamic characteristics of the non-stabilized oxygen-containing monolayer which reflects in the absence of any adsorption influence on the process.

On the other hand, when the film growth takes place by holding the potential at high positive values the oxygen-containing species involved in reaction (9b) may be able to reaccommodate, yielding an aged oxygen monolayer. Consequently, the film growth process and the oxygen evolution should occur with the main participation of steps (5)–(8), (9a), (9b), (10b) and (11b). The aged oxygen monolayer formed by reaction (9b) acts apparently as an inhibitor of the film growth process. Hence, the formation of the hydrated oxide film under the SWPS conditions is greater than that observed under potentiostatic growth.

It is noteworthy that during the electroreduction period of the SWPS the non-stabilized oxygen-containing monolayer yields a non-stabilized electroreduced platinum. This reaction promotes the penetration of oxygen atoms into the metal lattice.

The efficiency of the process has also to be related to the net amount of $PtO_n \cdot x H_2O$ which results during each cycle in the SWPS. This depends principally on the switching potentials of the SWPS and on the time the potential is held at these potential values. The E_u value should be within the potential range corresponding to the hydrated oxide film growth. On the other hand, the E_l value should be located in a potential region in which the total electroreduction of either the Pt(OH) or the Pt(O) layer occurs. However, such E_l value should correspond to a potential region in which an incomplete electroreduction of the hydrated oxide layer takes place, so a net growth of the film occurs.

The preliminary results obtained with gold and rhodium indicate that the above discussion, basically derived from the behaviour on platinum, also applies to those metals.

From the present results one concludes that the SWPS technique—under a properly chosen set of corresponding conditions—offers an interesting possibility of obtaining a reproducible controlled roughness factor of the electrode surface for platinum as well as for gold and rhodium. It appears, therefore, as a promising procedure for electrode material pretreatment, especially when comparing the kinetic characteristics of different electrocatalytic reactions.

ACKNOWLEDGEMENTS

INIFTA is sponsored by the Consejo Nacional de Investigaciones Científicas y Técnicas, the Universidad National de La Plata and the Comisión de Investigaciones Científicas (Provincia de Buenos Aires). This work is partially supported by the Regional Program for the Scientific and Technological Development of the Organization of American States.

REFERENCES

1 S Altmann and R H Busch, Trans Faraday Soc., 45 (1949) 720
2 K. Nagel and H Dietz, Electrochim Acta, 4 (1961) 1
3 A Frumkin, Electrochim Acta, 5 (1961) 265
4 S. Shibata, Bull. Chem Soc Jap., 36 (1963) 525
5 J.S Mayell and S.H. Langer, J. Electrochem. Soc., 111 (1964) 438
6 A. Kozawa, J. Electroanal. Chem., 8 (1964) 20
7 J.P. Hoare, Electrochim. Acta, 9 (1964) 599
8 S Gilman, Electrochim. Acta, 9 (1964) 1025.
9 E V. Kasatkin and A A Rakov, Electrochim. Acta, 10 (1965) 131
10 J.P Hoare, J Electrochem. Soc., 116 (1969) 612.
11 J.P. Hoare, J. Electrochem. Soc., 116 (1969) 1390
12 S D. James, J Electrochem. Soc., 116 (1969) 1681
13 T. Biegler and R. Woods, J. Electroanal. Chem , 20 (1969) 73

14 A A. Yakovleva and V.I. Veselovskii, Elektrokhimiya, 6 (1970) 967
15 Yu.M Tyurin and G.F. Volodin, Elektrokhimiya, 6 (1970) 1186.
16 Yu M Tyurin, G.N. Afon'shin, G.F Volodin and V E Goncharuk, Elektrokhimiya, 6 (1970) 1854.
17 T. Biegler, D.A J. Rand and R. Woods, J Electroanal. Chem., 29 (1971) 269
18 S. Shibata and M P. Sumino, Electrochim Acta, 16 (1971) 1089.
19 J Balej and O. Spalek, Collect. Czech. Chem. Commun., 37 (1972) 499.
20 S. Shibata, Electrochim. Acta, 17 (1972) 395.
21 O Spalek and J Balej, Collect. Czech. Chem Commun., 38 (1973) 29
22 O Spalek and J Balej, Collect Czech. Chem. Commun., 38 (1973) 3715
23 B.Z. Nikolic, I.V Kadija and A.R. Despic, Bull. Soc. Chim. Beogr , 39 (1974) 453
24 W C. Johnson and L.A. Heldt, J. Electrochem. Soc., 121 (1974) 34
25 J.P. Hoare, J. Electrochem. Soc , 121 (1979) 872
26 W. Visscher and M Blijlevens, Electrochim Acta, 19 (1974) 387
27 J.F. Llopis and F Colom in A.J. Bard (Ed.), Encyclopedia of Electrochemistry of the Elements, Vol 6, Marcel Dekker, New York, 1976, p. 208.
28 J S. Hammond and N. Winograd, J. Electroanal. Chem., 78 (1977) 55
29 B.Z. Nikolic, A.R. Despic and R R. Adzic, Bull Soc Chim Beogr , 45 (1980) 9.
30 B.Z. Nikolic, A R. Despic and R.R. Adzic, Bull Soc. Chim Beogr , 45 (1980) 185.
31 J P Hoare, J. Electrochem. Soc., 127 (1980) 1758.
32 S. Shibata and M.P. Sumino, Electrochim Acta, 26 (1981) 517
33 S. Shibata and M.P Sumino, Electrochim Acta, 26 (1981) 1587
34 R. Woods in A.J. Bard (Ed.), Electroanalytical Chemistry, Vol. 9, Arnold Press, London, 1977, p 2
35 G. Bélanger and A.K. Vijh in A.K. Vijh (Ed)., Oxides and Oxide Films, Vol. 5, Marcel Dekker, New York, 1977, p. 2
36 M E. Folquer, J.O. Zerbino, N R. de Tacconi and A J. Arvia, J. Electrochem. Soc., 126 (1979) 592.
37 M.E. Folquer, N.R de Tacconi and A.J Arvia, J. Electrochem Soc , in press.
38 J.P Hoare, S.G. Meibuhr and R. Thacker, J Electrochem Soc., 113 (1966) 1078.
39 J.P. Hoare, R. Thacker and C.R. Wiese, J Electroanal. Chem , 30 (1971) 15
40 J.P. Hoare, Electrochim. Acta, 26 (1981) 225.
41 S M. Piovano, A.C. Chialvo, W E Triaca and A.J Arvia, in preparation.
42 J Van Muylder, N. de Zoubov and M. Pourbaix in M. Pourbaix (Ed.), Atlas of Electrochemical Equilibria in Aqueous Solutions, Pergamon Press, Oxford, 1966, p 379
43 B E Conway, H Angerstein-Kozlowska, F.C. Ho, J Klinger, B. Mac Dougall and S. Gottesfeld, Faraday Discuss. Chem. Soc., 56 (1973) 210
44 V.A. Lunenck-Burmakina, A P Potemskaya and A I Brodskii, Dokl. Akad. Nauk S.S S.R., 137 (1961) 1402.